Proceedings of the ASME 2021
International Design Engineering Technical Conferences &
Computers and Information in Engineering Conference
IDETC/CIE 2021
August 17-20, 2021, Virtual Conference, Online

DETC2021-71304

CO-DESIGN OPTIMIZATION OF A COMBINED HEAT AND POWER HYBRID ENERGY SYSTEM

Dongze Li[1], Jiaxin Wu[1], Jie Zhang[2], and Pingfeng Wang[1,*]

[1]Industrial and Enterprise Systems Engineering, University of Illinois at Urbana-Champaign, Urbana, IL, USA
[2]Mechanical Engineering, University of Texas at Dallas, Richardson, TX, USA

ABSTRACT

As an energy efficient technology that generates electricity and captures the heat that would otherwise be wasted to provide useful thermal energy, combined heat and power (CHP) hybrid energy systems have been widely used in the U.S. In the presented study, a two-stage co-design optimization model for CHP-based hybrid energy systems is developed. By applying a mixed integer programming (MIP) method, the optimization is performed from the operational and design perspectives. Six components: CHP, boiler, heat recover unit (HRU), thermal storage system (TS), power storage system (ES), and photovoltaic (PV) are considered in the CHP-based microgrids. During the optimization process, the cost-based optimal component design solutions are firstly obtained by minimizing the total installation costs of the components. The optimal operational strategy is further attained based on the component design by minimizing the costs from production, operation and maintenance, startup, and unsatisfied load. In the end, non-disruptive and disruptive scenarios are considered in the case study to testify to the model's effectiveness in co-design and reliability improvement.

Keywords: co-design optimization, microgrid, power and thermal management, disruptive scenarios

NOMENCLATURE

Parameters

c_{fuel}	Fuel price
$P^{CHP}_{\max}$,$P^{PV}_{\max}$	Maximum power generation capability of CHP, PV
$Q^{CHP}_{\max}$,$Q^{boil}_{\max}$,$Q^{HRU}_{\max}$	Maximum heat generation capability of CHP, boiler, HRU
$E^{TS}_{\max}$,$E^{ES}_{\max}$	Maximum state of charge of TS, ES
$E^{TS}_{\min}$,$E^{ES}_{\min}$	Minimum state of charge of TS, ES
$Q^{c}_{\max}$,$Q^{d}_{\max}$	Maximum heat charging and discharging rate TS
$P^{c}_{\max}$,$P^{d}_{\max}$	Maximum electric charging and discharging rate of ES
η^{CHP}	Power generation efficiency of CHP
η^{boil}	Heat generation efficiency of boiler
η^{CHP}_{loss},η^{TS}_{loss}	Heat loss efficiency of CHP, TS
η^{HRU}	Heat recover efficiency of HRU
η^{cvt}	Converter power transformation efficiency
η^{TS}_{c},η^{ES}_{c}	Charge efficiency of TS, ES
η^{TS}_{d},η^{ES}_{d}	Disharge efficiency of TS, ES
$Ru^{CHP}_{\max}$,$Ru^{boil}_{\max}$	Ramp up rate limit of CHP, boiler
$Rd^{CHP}_{\max}$,$Rd^{boil}_{\max}$	Ramp down rate limit of CHP, boiler
C^{CHP}_{s},C^{boil}_{s},C^{HRU}_{s}	Startup costs of CHP, boiler, and HRU
C^{TS}_{s},C^{ES}_{s},C^{PV}_{s}	Startup costs of TS, ES, and PV
C^{CHP}_{OM},C^{boil}_{OM},C^{HRU}_{OM}	Operation and maintenance costs of CHP, boiler, and HRU
C^{TS}_{OM},C^{ES}_{OM},C^{PV}_{OM}	Operation and maintenance costs of TS, ES, and PV
C^{CHP}_{inst},C^{boil}_{inst},C^{HRU}_{inst}	Installation costs of CHP, boiler, and HRU
C^{TS}_{inst},C^{ES}_{inst},C^{PV}_{inst}	Installation costs of TS, ES, and PV
c_{ue},c_{uq}	Unsatisfied power and heat load prices
C_{oper},C_{inst}	Overall operational and installation costs

Variables

P^{CHP}_{t},P^{PV}_{t}	Power generated by CHP and PV at t
P^{c}_{t},P^{d}_{t}	Power charged or discharged in ES at t
Q^{CHP}_{t},Q^{boil}_{t}	Heat generated by CHP and boiler at t
Q^{c}_{t},Q^{d}_{t}	Heat charged or discharged in TS at t
μ^{c}_{t},μ^{d}_{t},ω^{c}_{t},ω^{d}_{t}	Binary variables indicating charging and dis charging state for ES, TS
θ_t, γ_t, λ_t, δ_t, α_t, β_t	Binary variables indicating the status of CHP, boiler, HRU, TS, ES, PV
St^{CHP}_{t},St^{boil}_{t},St^{HRU}_{t}	Binary variables indicating startup state of CHP, boiler, and HRU
St^{TS}_{t}, St^{ES}_{t}, St^{PV}_{t}	Binary variables indicating startup state of TS, ES, and PV

*Corresponding author: pingfeng@illinois.edu
DETC conf paper: version 1.26, May 21, 2021

E_t^{TS}, E_t^{ES}	State of charge for TS, ES at t
C_t^{CHP}, C_t^{boil}, C_t^{HRU}	Costs from CHP, boiler, and HRU at t
C_t^{TS}, C_t^{ES}, C_t^{PV}	Costs from TS, ES, and PV at t
C_t^{pena}	Costs from unsatisfied power and heat load at t
u_t^e, u_t^q	Unsatisfied electrical, heat demands at t

1. INTRODUCTION

To date, a majority of the total energy consumed in the United States to heat homes, run vehicles, power industry and manufacturing, and provide electricity, has been generated from fossil fuels such as oil, coal, and natural gas. Eventually, the degree to which the society depends on fossil fuels will have to decline as the supplies diminish, the cost of tapping remaining reserves increase, and the effect of their continued use grows more critically. To tackle these problems, more efficient and environmentally friendly energy production systems have been widely studied in the literature [1, 2]. One of the technologies being proposed is combined heat and power (CHP) systems, which combine the heat engine and the power plant to generate electricity and heat resources simultaneously [3]. The CHP has been considered as one of the most cost-efficient methods for reducing carbon emissions in heating systems [4], and also recognized to be the most energy efficient method of transforming energy from fossil fuels or biomass into electric power [5, 6]. Therefore, numerous applications in the fields of farming, industrial powering, and residential buildings have applied the CHP technology [7–9]. A detailed introduction about components of the CHP system as well as their corresponding technology characterizations has been provided by Darrow et al. [6] from the U.S Environmental Protection Agency. While the application of CHP systems could potentially provide significant benefits in improving energy efficiency and environmental sustainability, the design of CHP systems to optimally integrate different systems components and their operational control strategies simultaneously for enhanced system performances and resilience, especially in the event of system disruptions, remains a grand challenge to be addressed.

One of the CHP applications is in microgrids (MGs), which can efficiently integrate various types of distributed energy sources, especially renewable energy sources (RESs), to fulfill different operational requirements and enhance the overall system flexibility and reliability [10, 11]. More information for detailed models of components as well as the layouts for MGs can be found in the related literature [12, 13]. Recently, a study of CHP based MG system that includes CHP units in the grid has been reported and attracts great interests [14]. Although the CHP based MG system can effectively satisfy both thermal and power demands by simultaneously generating heat and power resources, the interdependency among key system components due to the co-generation behavior on the other hand can significantly limit the system's flexibility and resilience to disruptive events. Therefore, additional grid components providing ancillary service are often required to enhance the co-generation flexibility and reliability of the system. These additional grid components may include the heat recovery unit (HRU), boiler, the thermal storage system (TS), and the power storage system (ES). Moreover, MGs can utilize RES such as photovoltaic (PV) panels to make the heat and power production more environmentally friendly and cost effective [15–18]. However, adding additional grid components into the MG system will increase the system complexity, making it more difficult for the operations control and management. For example, with an increased system complexity, it will be more challenging for system operators to find an optimal production plan that maximizes the economic and environmental benefits. Hence, an effective operations management system for scheduling different resources under operational constraints is crucially needed to accomplish the system objective. In addition to the challenges in operations, complex interdependence among different components of an MG makes it vulnerable towards external disruptions. Consequently, how to mitigate the negative impacts of potential disruptive events is an important yet challenging task during the design stage to improve the resilience and reliability of CHP based MGs. Wang et al. [19] presented a comprehensive review on resilience-oriented modeling and operational strategies for MGs. Extensive studies have also been conducted on resilience modeling, quantification, control and optimization [20–25]. Additionally, Hu et al. [26] conducted the study of using different control strategies to optimize the system design with an emphasis on improving system reliability. Wu and Wang [27] compared different control strategies for enhancing system's resilience when undergoing disruptions. Moreover, different recovery methods have been identified optimally to improve the grids' resilience after disruptions by deploying resources proactively [28, 29].

Besides resilience against system disruptions, studies have also been reported in the literature to analyze the performance of CHPs with respect to the installation and operation costs while satisfying energy demands. Zafarani et al. [30] and Odonkor et al. [31, 32] presented the study of robust operation of a multicarrier energy system (MES), which share the same characteristic as a CHP unit. Apart from the operation, the design of an MG system such as sizing of key system components can affect not only the initial installation costs but also the overall energy production performance and operation and maintenance (O&M) costs. For instance, if the capacity of a boiler is not adequately installed, the MG could potentially not be able to satisfy the heat demand during the peak hours. In the contrast, there will be unnecessary installation and O&M costs if the boiler's capacity is designed to be excessive. To facilitate the design of the CHP based MG system, models for different system components have been derived from the collected historic data [33, 34], which take into account variations in the performances and costs as induced by different ratings and operating conditions. The overall costs of the CHP based MG system including both installation and operating costs would depend on the system design as well as the operational controls.

Although studies have been conducted separately at the MG design stage or the operational control stage to enhance its performances, without considering the couplings between the MG system designs and operation controls holistically, they usually produce suboptimal results with low reliability and economic efficiency. Thus, to address the challenge and further enhance resilience and economical efficiency of the CHP based MGs, this

paper presents a co-design framework that integrates the system component designs with their operational control optimization while considering potential disruptive scenarios in advance. Co-design has been widely used in solving multidisciplinary design optimization (MDO) problems [35]. Cui et al. [36] compared design formulations and problem-solving strategies for better solving reliability-based co-design problems. Nash et al. [37] presented a model fidelity-based decomposition (MFBD) hierarchical control co-design (HCCD) algorithm designed to optimize system performance characteristics. Liu et al. [38] formulated two decentralized approaches to solve multisubsystem co-design problems. In this paper, we propose a two-stage co-design optimization model to identify not only the optimal designs but also the optimal operation management strategies of an CHP based MG system. To validate the effectiveness of the developed co-design methodology in improving system resilience and cost efficiency, a case study has been conducted that evaluates the system design performances under different scenarios, with and without external disruptions.

The rest of the paper is organized as follows: Sec. 2 presents the developed co-design optimization model for CHP-based MGs, Sec. 3 evaluates the developed co-design methodology with a design case study considering different operating conditions, and Sec. 4 concludes the study with brief discussions on the effectiveness of the developed co-design methodology.

2. CO-DESIGN MODEL FOR CHP-BASED MGS

The co-design methodology developed in this paper consists of two interdependent optimization sub-problems: the optimal operations control of the CHP-based MG system and the optimal design of the CHP-based MG system with configurations of key system components. The objective is to minimize the total cost of the CHP-based MG system which includes the production costs, O&M costs, startup costs, and extra penalty costs from unsatisfied power and heat demands. As for the first optimization sub-problem, we will consider the optimal operations control of the CHP components for a given MG system design, such as scheduling on-off state of components, the generations of heat and power, and controlling the state of charge of the energy storage system to minimize the cost. For the second optimization sub-problem, it is intended to optimize the specific design parameters of the key components of the CHP based MG system such as the installation ratings and storage capacities, which will in turn affect the optimal operations control in the first optimization sub-problem. Since optimums of system operations control parameters in the first optimization sub-problem and system design parameters in the second one are dependents, they can be derived iteratively through solving these two sub-optimization problems jointly as a whole. Since the design and operations control parameters are associated with different cost items in the total cost, the goal of the co-design model is thus to find the most cost-effective solutions while considering different design and operation constraints, as shown in Eqn. (1) below.

$$\min C_{oper} + C_{inst} \tag{1}$$

Overall, the co-design optimization problem is nonlinear and discrete, and therefore can be viewed as a MIP model. The 'branch and cut ' [39] algorithm is applied to solve the optimization in Gurobi optimizer [40]. The developed co-design methodology is further detailed in the following sections.

2.1 Heat and Power Scheduling Optimization

The CHP-based MG model in this paper mainly consists of six components: CHP, boiler, HRU, TS, ES, and PV as shown in Fig. 1. In the configuration, the solar irradiation will be absorbed by the PV system to generate electrical power, which can be stored in the ES and further used to serve the electric demands after going through DC/AC by converters. On the other hand, the CHP subsystem transfers energy from fuels into heat and electricity simultaneously. The excessive electricity generated from the CHP can also be stored in the ES, while the heat will be delivered into the HRU with inevitable thermal losses. The HRU can then transfer the heat into useful thermal energy, which can be stored in the TS and further used to serve the thermal demands. Additionally, the boiler can also be used to generate useful thermal energy from fuels directly, in case the production from the CHP cannot satisfy the thermal demands in the system. Note that the heat stored in the TS in this configuration, unlike ES, will be lost gradually as time goes on. With all these heterogeneous

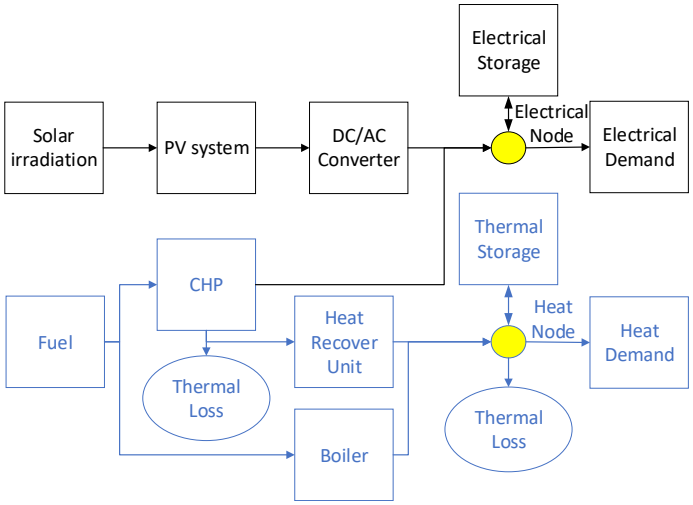

FIGURE 1: CONFIGURATION OF A CHP-BASED MG MODEL

components in the CHP based MG system, there is a need to find the optimal combination of those components to minimize the daily production cost. The objective function for such daily cost can be hourly summarized in Eqn. (2):

$$\min C_{oper} = \sum_{t=1}^{24} (C_t^{CHP} + C_t^{boil} + C_t^{HRU} + C_t^{TS} + C_t^{ES} + C_t^{PV} + C_t^{pena}), \tag{2}$$

where the total operation cost to be minimized includes startup and O&M costs of each of these key components. Additionally, unsatisfied heat and electricity demands will be penalized by including an extra cost item in the total cost. Furthermore, Eqns. (3)-(7) show how to calculate the operational cost of each individual component. For the cost from CHP and boiler in Eqns. (3)-(4), the first term represents the fuel consumption cost;

the second term indicates the costs from operation and maintenance; the third term is the startup cost of the component. The cost items shown in Eqns. (5)-(8) only depend on O&M and startup process decisions, since the respective components do not consume fuels in operation. Lastly, the cost resulted from unsatisfied loads is characterized in Eqn. (9).

$$C_t^{CHP} = c_{fuel}\frac{P_t^{CHP}}{\eta^{CHP}} + \theta_t C_{OM}^{CHP} + St_t^{CHP} C_s^{CHP}, \tag{3}$$

$$C_t^{boil} = c_{fuel}\frac{Q_t^{boil}}{\eta^{boil}} + \gamma_t C_{OM}^{boil} + St_t^{boil} C_s^{boil}, \tag{4}$$

$$C_t^{HRU} = \lambda_t C_{O\&M}^{HRU} + St_t^{HRU} C_s^{HRU}, \tag{5}$$

$$C_t^{TS} = \delta_t C_{O\&M}^{TS} + St_t^{TS} C_s^{TS}, \tag{6}$$

$$C_t^{ES} = \delta_t C_{O\&M}^{ES} + St_t^{TS} C_s^{ES}, \tag{7}$$

$$C_t^{PV} = \beta_t C_{O\&M}^{PV} + St_t^{PV} C_s^{PV}, \tag{8}$$

$$C_t^{pena} = c_{ue} u_t^e + c_{uq} u_t^q. \tag{9}$$

The operation of the CHP is controlled by Eqns. (10)-(13), where Eqn. (10) calculates the useful heat recovered from the HRU; Eqns (11) and (12) introduce the predefined limit of power and heat generated by CHP, respectively. Moreover, as generators are typically restricted on their ramp up and ramp down rates for power generation in practical applications, these constraints are correspondingly implemented in Eqn. (13). While the power and heat generations are correlated in the CHP and the heat is passively produced, considering the ramping rates for heat generation is often not necessary. More details for the formulations of the CHP can be found in [41].

$$Q_t^{CHP} = \frac{P_t^{CHP}}{\eta^{CHP}}(1-\eta^{CHP}-\eta_{loss}^{CHP})\eta^{HRU}, \tag{10}$$

$$0 \le P_t^{CHP} \le P_{\max}^{CHP}, \tag{11}$$

$$0 \le Q_t^{CHP} \le Q_{\max}^{CHP}, \tag{12}$$

$$Rd_{\max}^{CHP} \le \frac{P_t^{CHP} - P_{t-1}^{CHP}}{t-(t-1)} \le Ru_{\max}^{CHP}. \tag{13}$$

Besides operating the CHP, we also need to consider the ON/OFF status of each component in the MG. All six components considered can either be enabled or disabled at every moment to fulfill different operating conditions. Enable a component requires additional operational and maintenance costs. Therefore, it will be beneficial to switch off any component to reduce the overall cost if the generation is excessive in the MG. For instance, if the PV and the boiler can meet the requirement of power and heat demand at time t in a more costs-effective way, then the CHP can be disabled to cut down costs. And Eqn. (14) encodes this logic for operational status switching:

$$P_t^{CHP} \le \theta_t A, \tag{14}$$

where θ_t is a binary control variable for CHP. CHP is enabled when θ_t equals to 1, and it is disabled otherwise. Nonetheless, switching the component on and off cannot be performed arbitrarily without any cost. Whenever the components are started, additional startup costs due to extra energy consumption are imposed. And this cost prevents all components from restarting too frequently during the operation. Instead, the optimal scheduling is needed to determine when and which component is enabled or disabled at each time step. The relationship between the status variable θ_i and the startup decision variable St_t^{CHP} can be described in Eqn. (15). This equation is used to determine whether the CHP is enabled at time t. If $\theta_t - \theta_{t-1} = 1$, then the CHP has been restarted and the corresponding startup cost shows up. Otherwise the CHP is not enabled and $St_t^{CHP} = 0$ at time step t.

$$\begin{aligned} &\theta_t - \theta_{t-1} \le St_t^{CHP}, \\ &(\theta_t - \theta_{t-1} - 1) \times St_t^{CHP} = 0. \end{aligned} \tag{15}$$

Moreover, Eqns. (16) and (17) introduce the lower/upper bound of the heat generation and the ramping rate for the boiler, respectively. Equation. (18) controls the output from boiler by incorporating a binary status indicator γ_i. And similiar to Eqn. (15), Eqn. (19) determines whether to start the boiler at time step t based on the status variable γ_i.

$$0 \le Q_t^{boil} \le Q_{\max}^{boil}, \tag{16}$$

$$Rd_{\max}^{boil} \le \frac{Q_t^{boil} - Q_{t-1}^{boil}}{t-(t-1)} \le Ru_{\max}^{boil}, \tag{17}$$

$$Q_t^{boil} \le A\gamma_i, \tag{18}$$

$$\begin{aligned} &\gamma_t - \gamma_{t-1} \le St_t^{boil}, \\ &(\gamma_t - \gamma_{t-1} - 1) \times St_t^{boler} = 0 \end{aligned} \tag{19}$$

Furthermore, for HRU, Eqns. (20)-(22) model the HRU's capacity, on-off status, and startup decisions, respectively.

$$0 \le Q_t^{HRU} \le Q_{\max}^{HRU}, \tag{20}$$

$$Q_t^{HRU} \le A\lambda_i, \tag{21}$$

$$\begin{aligned} &\lambda_t - \lambda_{t-1} \le St_t^{HRU}, \\ &(\lambda_t - \lambda_{t-1} - 1) \times St_t^{HRU} = 0 \end{aligned} \tag{22}$$

So far we have introduced the modeling for CHP, boiler, and HRU units in the MG. To improve the efficiency of utilizing heat and power resources, additional TS and ES can be installed in the system. Based on the modeling of TS and ES developed in [42], this paper formulates constraints for operating the TS and ES by considering their on-off status, operation/maintenance and startup costs. As for TS, the corresponding operational condition is determined by Eqn. (23), where the SOC in the next time step E_{t+1}^{TS} depends on the current SOC, the heat flow in and out, and the heat loss rate with predefined efficiency constant. Equation (24) adds capacity constraints for the SOC of the TS to ensure the stability of the unit. Equation (25) provides the limit of the heat power charging and discharging rates within a given range. Moreover, Eqn. (26) indicates that the heat discharged from the TS cannot surpass the current SOC. And the TS cannot be charged and discharged at the same time as shown in Eqn. (27). By following Eqn. (28), we can only discharge/charge the TS when it is enabled. Lastly, Eqn. (29) derives the restart decisions for the TS during operations.

$$E_{t+1}^{TS} = (1-\eta_{loss}^{TS})E_t^{TS} + \eta_c^{TS}Q_t^c - Q_t^d/\eta_d^{TS}, \tag{23}$$

$$E_{\min}^{TS} \le E_t^{TS} \le E_{\max}^{TS}, \tag{24}$$

$$\begin{aligned}\omega_t^c Q_{\min}^c \le Q_t^c \le \omega_t^c Q_{\max}^c,\\ \omega_t^d Q_{\min}^d \le Q_t^d \le \omega_t^d Q_{\max}^d,\end{aligned} \tag{25}$$

$$Q_t^d \le E_t^{TS}, \tag{26}$$

$$\omega_t^c + \omega_t^d \le 1, \tag{27}$$

$$\omega_t^c, \omega_t^d \le A\delta_t, \tag{28}$$

$$\begin{aligned}&\delta_t - \delta_{t-1} \le St_t^{TS},\\ &(\delta_t - \delta_{t-1} - 1) \times St_t^{TS} = 0.\end{aligned} \tag{29}$$

By modifying the formulations of the TS, the constraints of operating the ES are derived as shown in Eqns. (30)-(36). Note that the difference here as compared to Eqn. (23) is that the energy loss term, η_{loss}^{TS}, has been omitted because the fact that the electricity loss rate in ES is usually much smaller than the heat loss rate in TS in Eqn. (30).

$$E_{t+1}^{ES} = E_t^{ES} + \eta_c^{ES}P_t^c - P_t^d/\eta_d^{ES}, \tag{30}$$

$$E_{\min}^{ES} \le E_t^{ES} \le E_{\max}^{ES}, \tag{31}$$

$$\begin{aligned}\mu_t^c P_{\min}^c \le P_t^c \le \mu_t^c P_{\max}^c,\\ \mu_t^d P_{\min}^d \le P_t^d \le \mu_t^d P_{\max}^d,\end{aligned} \tag{32}$$

$$P_t^d \le E_t^{ES}, \tag{33}$$

$$\mu_t^c + \mu_t^d \le 1, \tag{34}$$

$$\mu_t^c, \mu_t^d \le A\alpha_t, \tag{35}$$

$$\begin{aligned}&\mu_t - \mu_{t-1} \le St_t^{ES},\\ &(\mu_t - \mu_{t-1} - 1) \times St_t^{ES} = 0.\end{aligned} \tag{36}$$

As for the PV unit, Eqns. (37)-(39) are used to control its capacity, on-off status, and startup decisions, respectively.

$$0 \le P_t^{PV} \le P_{\max}^{PV}, \tag{37}$$

$$P_t^{PV} \le A\beta_i, \tag{38}$$

$$\begin{aligned}&\beta_t - \beta_{t-1} \le St_t^{PV},\\ &(\beta_t - \beta_{t-1} - 1) \times St_t^{PV} = 0.\end{aligned} \tag{39}$$

In the co-design model, in addition to the formulations of operating the aforementioned components, we also need to optimally fulfill the heat and power demands. Thus, Eqns. (40) and (41) quantify any unsatisfied demand u_t^q and u_t^e in the MG. The heat load is served by the resources generated from the CHP, boiler, and TS, while the electrical load is served by the CHP, PV, and ES. During the online operation, if the total heat or power generation is not enough to satisfy the demand in the MG, then u_t^q or u_t^e will be positive and extra penalty costs can be calculated by Eqn. (9). As a result, purchasing commodities from the main grid to mitigate the shortage is required, which leads to additional costs as quantified in Eqn. (9).

$$D_t^Q - (Q_t^{CHP} + Q_t^{boil} + (Q_t^d - Q_t^c)) = u_t^q, \tag{40}$$

$$D_t^E - (P_t^{CHP} + \eta^{cvt}P_t^{PV} + (P_t^d - P_t^c)) = u_t^e. \tag{41}$$

It's noteworthy to mention that the formulations of Eqns. (40) and (41) enable the co-design model to consider both the nominal and disruptive operating scenarios for the CHP based MG system design. For example, sudden decrements in the CHP capacity can be related to the parameter Q_t^{CHP}, and changes in D_t^Q/D_t^E can also reflect the surge or dip in the heat/power demands. Hence in the case study, five disruptive scenarios are pre-considered together before optimization. With the considerations of potential disruptive scenarios, optimal solutions for designing the MG and scheduling the heat/power generations can be derived, and further make the system more resilient.

2.2 Components Design Optimization

While the formulation of the first optimization sub-problem in operations control has been discussed in Sec. 2.1, in this section the second optimization sub-problem for the CHP-based MG system design with heterogeneous components will be elaborated. Each of the six components has its own set of design parameters, which will significantly affect its performance in the operation stage. In this study, we need to optimize system design parameters which are associated with different system installation costs. And the installation cost is calculated according to Eqn. (42) based on the Min-Max normalization technique in [43]. The values of design parameters and component installation costs are all transferred from their given design spaces to a $[0, 1]$ range, and the installation cost for the component i, which is also normalized to be within the range $[0, 1]$, equals to the mean of all its parameters' values. In this formulation, we assume that all parameters are positively correlated with the installation cost, i.e. a larger capacity usually leads to a higher cost. For a component with several design parameters, we equally weight all parameters in the calculation of the final installation cost.

$$\frac{C_{inst}^{c_i} - C_{inst\_lb}^{c_i}}{C_{inst\_ub}^{c_i} - C_{inst\_lb}^{c_i}} = \frac{1}{n_i}\sum_{j=1}^{n_i}\frac{v_{ij} - v_{ij\_lb}}{v_{ij\_ub} - v_{ij\_lb}} \quad \forall i \in components, \tag{42}$$

where n_i is the number of design parameters of component i; v_{ij}, v_{ij_ub}, v_{ij_lb} are the design value, upper bound, and lower bound of the design parameter j for component i, respectively; $C_{inst}^{c_i}$, $C_{inst\_ub}^{c_i}$, $C_{inst\_lb}^{c_i}$ are the value, upper bound, and lower bound of installation cost for component i, respectively.

Taking the PV design as an example, there are a total of three design parameters to be considered. Each parameter is normalized to be within the interval of $[0, 1]$ by subtracting its lower limit and dividing its range. For example, if the design values of P_{max}^{PV}, C_s^{PV}, and C_{OM}^{PV} are $1150kW$, $\$18/h$, and $\$5/h$ respectively, and the design spaces for the three parameters are $(800-1500)kW$, $(\$10-\$30)/h$, and $(\$5-\$25)/h$, then the normalized values of the three parameters are 0.5, 0.4, and 0. Thus, after calculating the mean value of the three normalized values, we get the normalized result of C_{inst}^{PV} to be 0.3. Furthermore, if the cost range of C_{inst}^{PV} is within $(\$2000 - \$3000)$, then the C_{inst}^{PV} equals to \$2300 w.r.t the previous normalized result of 0.3.

Table 1 summarizes the parameters that can be designed for each component. There are 33 parameters in total while each parameter can be decided from a certain range. The installation cost of each component also has a predefined range, and can be calculated from Eqn. (42). Then, with all the formulations on

hand, we can optimize the co-design model to obtain the optimal design parameters as well as the scheduling for heat/power generations, by minimizing the overall cost shown in Eqn. (1).

TABLE 1: DESIGN PARAMETERS OF COMPONENTS IN THE MG

Components	Parameters
CHP	$P^{CHP}_{\max}, Q^{CHP}_{\max}, \eta^{CHP}, C^{CHP}_{s}, C^{CHP}_{OM}, Ru^{CHP}_{\max}, Rd^{CHP}_{\max}$
Boiler	$Q^{boil}_{\max}, \eta^{boil}, C^{boil}_{s}, C^{boil}_{OM}, Ru^{boil}_{\max}, Rd^{boil}_{\max}$
HRU	$\eta^{HRU}, C^{HRU}_{s}, C^{HRU}_{OM}$
TS	$E^{TS}_{\max}, \eta^{TS}_{c}, \eta^{TS}_{d}, Q^{c}_{\max}, Q^{d}_{\max}, C^{TS}_{s}, C^{TS}_{OM}$
ES	$E^{ES}_{\max}, \eta^{ES}_{c}, \eta^{ES}_{d}, P^{c}_{\max}, P^{d}_{\max}, C^{ES}_{s}, C^{ES}_{OM}$
PV	$P^{PV}_{\max}, C^{PV}_{s}, C^{PV}_{OM}$

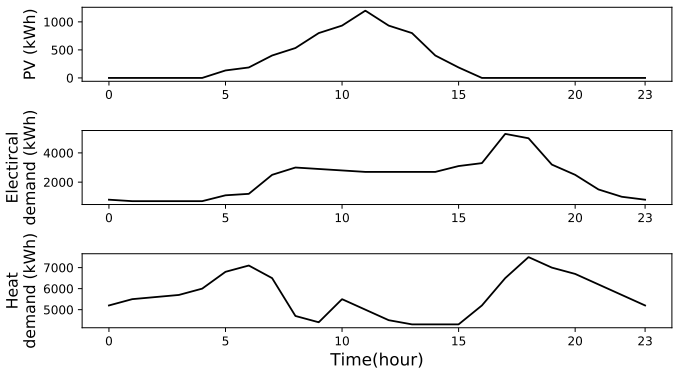

FIGURE 2: DAILY PV GENERATION, ELECTRICITY AND HEAT DEMAND USED IN THE CASE STUDY

3. CASE STUDY

To demonstrate the effectiveness of the proposed optimization model, we consider to control the operations as well as to optimize the design of a CHP based MG with a layout shown in Fig. 1. Figure 2 summarizes the data used in the case study, including the daily heat and electrical loads as well as the PV generation in the MG. The energy demand data is adopted from [41].

Table 2 shows the values of each parameter and the range of the installation cost of each component as well as other constants used in the optimization model. The CHP considered in this study relies on the reciprocating engine technology, and corresponding parameters' specifications are adopted from [6, 44]. The settings of parameters of the HRU, boiler, TS, ES as well as the PV are adopted from the studies in [6, 44–47]. The initial SoC for TS/ES is set to be $0.8/0.3$ correspondingly. The co-design simulation model is formulated as an MIP model and solved by the Gurobi optimizer [40] with the Python API. We first consider an operating scenario without any external disruptions followed by the case study on the same CHP based MG with disruptive events injected during the operation. Simulation results demonstrate that the proposed co-optimization model is applicable for the MG in both scenarios.

TABLE 2: DESIGN SCOPE AND SPECIFIC VALUE OF PARAMETERS

Parameters	Ranges or Values	Parameters	Ranges or Values
$P^{CHP}_{\max}$	4000-6000 kW	$Q^{CHP}_{\max}$	4000-6000 kW
η^{CHP}	0.27-0.41	C^{CHP}_{s}	\$10-\$30/h
C^{CHP}_{OM}	\$5-\$25/h	$Ru^{CHP}_{\max}$	500-1500 kW/h
$Rd^{CHP}_{\max}$	500-1500 kW/h	$Q^{boil}_{\max}$	4000-6000 kW
η^{boil}	0.7-0.8	C^{boil}_{s}	\$10-\$30/h
C^{boil}_{OM}	\$5-\$25/h	$Ru^{boil}_{\max}$	1000-3000 kW/h
$Rd^{boil}_{\max}$	1000-3000 kW/h	η^{HRU}	0.7-0.8
C^{HRU}_{s}	\$10-\$30/h	C^{HRU}_{OM}	\$5-\$25/h
$E^{TS}_{\max}$	1200-3200 kWh	η^{TS}_{c}	0.9-0.95
η^{TS}_{d}	0.9-0.95	$Q^{c}_{\max}$	500-1000 kW
$Q^{d}_{\max}$	500-1000	C^{TS}_{s}	\$10-\$30/h
C^{TS}_{OM}	\$5-\$25/h	$E^{ES}_{\max}$	1000-3000 kWh
η^{ES}_{c}	0.9-0.95	η^{ES}_{d}	0.9-0.95
$P^{c}_{\max}$	300-1000 kW	$P^{d}_{\max}$	300-1000 kW
C^{ES}_{s}	\$10-\$30/h	C^{ES}_{OM}	\$5-\$25/h
$P^{PV}_{\max}$	800-1500 kW	C^{PV}_{s}	\$10-\$30/h
C^{PV}_{OM}	\$5-\$25/h	A	100000
c_{fuel}	\$0.49/h	η^{TS}_{loss}	0.05
η^{CHP}_{loss}	0.01	η^{CHP}	0.9
c_{ue}	\$40/kWh	c_{uq}	\$40/kWh
E^{TS}_{0}	$0.8E^{TS}_{\max}$	E^{ES}_{0}	$0.3E^{ES}_{\max}$
C^{CHP}_{inst}	\$1,500-\$2,900	C^{boil}_{inst}	\$3,000-\$4,500
C^{HRU}_{inst}	\$500-\$1,000	C^{TS}_{inst}	\$3,000-\$4,500
C^{ES}_{inst}	\$3,000-\$4,500	C^{PV}_{inst}	\$2,000-\$3,000

3.1 Results Under Non-disruptive Scenario

First we solve the optimization model introduced in Sec. 2 without considering any component outage. The co-optimization model is first parameteraized by the values shown in Table 2. The model is solved to satisfy the loads as shown in Fig. 2. The corresponding optimal solutions of the parameters of each component are derived and shown in Table 3. Based on the results of these design parameters, the optimal installation cost C_{inst} can be found as \$15, 305, after solving Eqn. (42). Notice that, results shown in Table 3 indicate that the optimal solutions of the operation/maintenance cost and the startup cost are at the minimum level within the predefined parameter range. This observation means that obtaining the lowest cost for both operation and installation at the same time is preferable during the component design stage. From the numerical results, another observation is that the the heat generation efficiency of the boiler and the heat recovery efficiency of the HRU are designed to be the largest value from their given ranges. This is a realization of the trade-off between the installation cost and the online operational cost, i.e., a component with a lager capacity requires more initial investment but is less prone to cause energy shortages or frequent restarting. Thus, simulation results suggest that the benefits of having

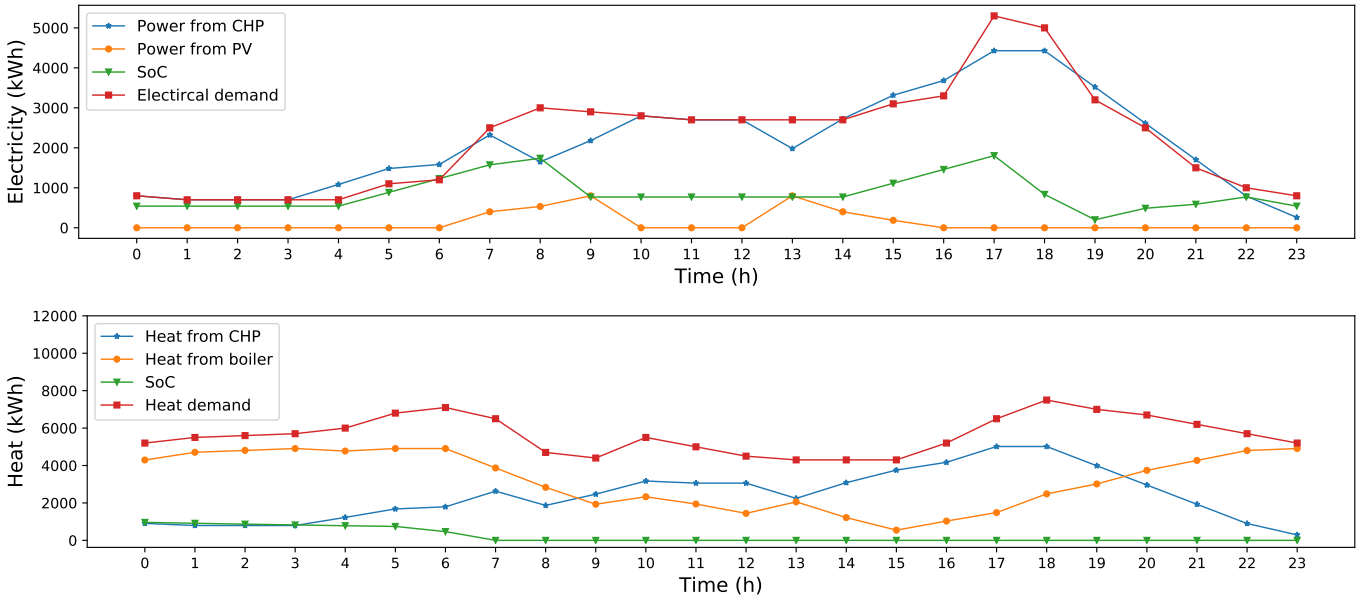

FIGURE 3: ELECTRICAL AND THERMAL DEMAND, PRODUCTION, STORAGE STATUS IN THE CHP BASED MG.

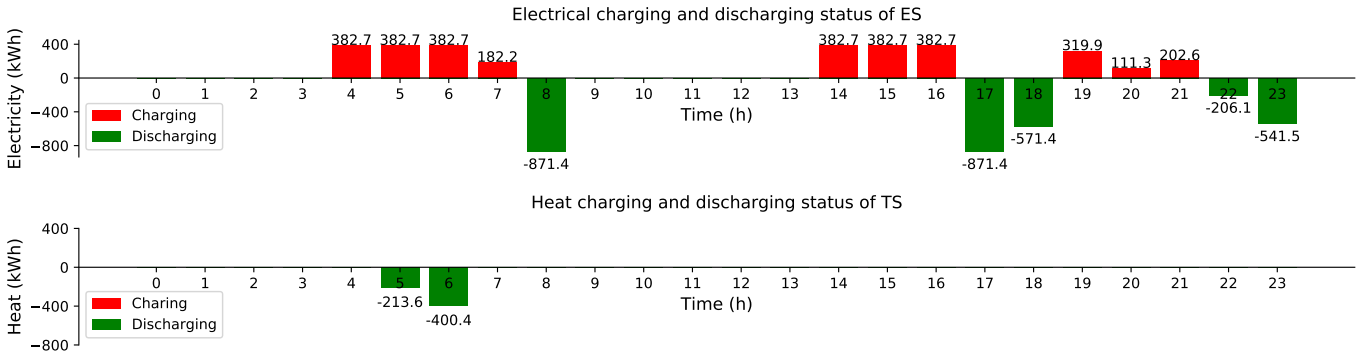

FIGURE 4: CHARGING AND DISCHARGING STATUS OF ES AND TS.

efficient boiler and HRU outperform the higher initial fixed cost from setting up such units in the CHP based MG.

As for the case study results during the operational stage, Fig. 3 shows the dynamic power/heat demand, the power/heat generation from CHP, boiler, PV, and the SOC of the TS/ES unit. In this study, we consider an operation horizon of 24 times steps to simulate the system performance spanning one day. Results in Fig. 3 are the solutions for optimally scheduling the power/heat generation from different components given the specific design parameters shown in Table 3. As a result, the daily optimal operational cost C_{oper} is found to be $\$11,331.2$. To analyze the behavior of the energy storage units, Fig. 4 illustrates the charging and discharging status of the ES and TS units. Recall that the initial SOC for the ES and TS at time 0 is set to be 0.3 and 0.8, respectively. It is seen from Fig. 4 that the TS only discharges heat during the daytime, while the heat from the TS and boiler together satisfies the heat demand that cannot be met by the CHP. In the contrast, the ES charging and discharging frequency is higher. This may due to the large amplitude variance of the electrical demand during the day. On the other hand, Fig. 5 shows the detailed on-off status of all six components in the CHP based MG. At each time step, the grey block means that the component is enabled, while the white block indicates the component is disabled. Based on the status results, the CHP, boiler, and HRU are enabled through the whole simulation time span (one day), while TS, ES, and PV are disabled intermittently.

To summarize, from results of the system performance shown in Fig. 3, the heat and power loads can be completely satisfied in the MG that is designed based on the co-design method. By analyzing the trends of the generations and demands in the MG, it is found that the generating units, e.g. the CHP, boiler, and PV, have optimally adjusted their outputs to minimize the operating cost. And the total cost of such a CHP based MG including both the design cost and the operational cost in one day is $\$26,636.2$ based on Eqn. (1).

In order to verify the effectiveness of the co-design optimization model, we further choose the middle value of the design range for each parameter in Table 2 as the initial design and perform optimization. Because of page limit, we will not show visualized results of the initial design. The installation cost C_{inst} is

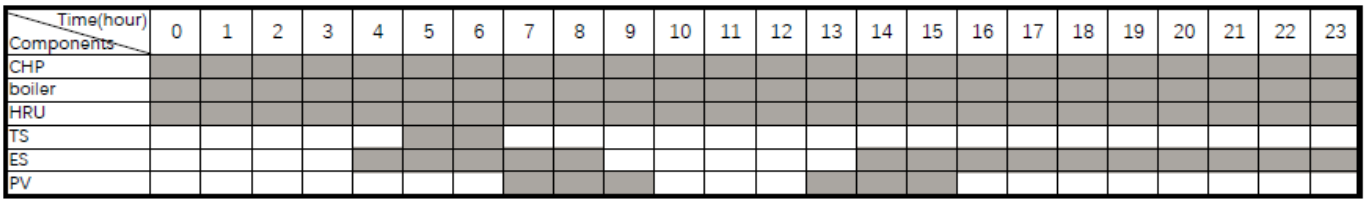

FIGURE 5: ON-OFF STATUS OF THE COMPONENTS.

TABLE 3: OPTIMAL DESIGN SOLUTIONS UNDER THE NON-DISRUPTIVE SCENARIO

Parameter	Optimal Value	Parameter	Optimal Value
$P_{\max}^{CHP}$	4428.6 kW	η_c^{TS}	0.9
$Q_{\max}^{CHP}$	5015.3 kW	η_d^{TS}	0.9
η^{CHP}	0.41	$Q_{\max}^{c}$	500 kW
C_s^{CHP}	\$10/h	$Q_{\max}^{d}$	500
C_{OM}^{CHP}	\$5/h	C_s^{TS}	\$10/h
$Ru_{\max}^{CHP}$	745.9 kW/h	C_{OM}^{TS}	\$5/h
$Rd_{\max}^{CHP}$	908.7 kW/h	$E_{\max}^{ES}$	1803.1 kWh
$Q_{\max}^{boil}$	4907.3 kW	η_c^{ES}	0.9
η^{boil}	0.8	η_d^{ES}	0.9
C_s^{boil}	\$10/h	$P_{\max}^{c}$	382.7 kW
C_{OM}^{boil}	\$5/h	$P_{\max}^{d}$	871.4 kW
$Ru_{\max}^{boil}$	1000 kW/h	C_s^{ES}	\$10/h
$Rd_{\max}^{boil}$	1037.1 kW/h	C_{OM}^{ES}	\$5/h
η^{HRU}	0.8	$P_{\max}^{PV}$	800 kW
C_s^{HRU}	\$10/h	C_s^{PV}	\$10/h
C_{OM}^{HRU}	\$5/h	C_{OM}^{PV}	\$5/h
$E_{\max}^{TS}$	1200 kWh		

\$17991.7, and the daily optimal operational cost C_{oper} is found to be \$12578.4, which are both higher than the corresponding costs derived from the optimization. Most importantly, 1527.47 kWh unsatisfied load will be produced when applying the initial design. The unsatisfied load will result in a great loss according to Eqn. (9). In the end, the total cost of the initial design is \$91668.9, which is a lot more higher than \$26636.2, the optimal cost obtained from the co-design optimization.

3.2 Results Under Disruptive Scenarios

In Sec 3.1, we have demonstrated the results for the system during both the design and operational stage with the assumption of a perfect operating condition. However, disruptive events are hard to avoid for the power and heat generation process in practice. For instance, the demand in the system can be challenging to predict, and unpredicted outages can happen in any component in the MG. Thus, to access the system capability of handling external disruptive events, the co-design model is solved again considering following five disruptive events occurring during the operation.

- PV fails between the time steps 6 – 9.
- The CHP capacity is down to 50% between hour 14 – 16.
- The electrical load increases by 80% between hour 12 – 13.
- TS cannot discharge between hours 5 – 6.
- ES is disabled between hours 12 – 14.

After simulating all the disruptions, Table 4 summarizes the optimal solutions of the design parameters when such disruptions have been taken into account. And the optimal installation cost C_{inst} is found to be \$15, 990.4, based on the chosen design parameters of each component in this case. Moreover, the operation/maintenance cost and startup cost are solved to be at the minimum value of their predefined ranges. This observation of choosing the minimum is the same in the non-disruptive scenario. However, the optimal heat recovery efficiency is designed to be 0.76, which is lower than the case without any disruption. This may suggests that the additional installation cost of having more efficient HRU unit is not negligible, comparing to the benefit of having a better HRU during the online operation. Note that allocated capacities of the CHP and the boiler are larger when we take disruptive events into consideration. And this result indicates that greater capacities of generators can improve the system's resilience by introducing redundancy to the system.

TABLE 4: OPTIMAL DESIGN SOLUTION UNDER DISRUPTIVE SCENARIOS

Parameters	Optimal Values	Parameters	Optimal Values
$P_{\max}^{CHP}$	5600 kW	$Q_{\max}^{CHP}$	6000 kW
η^{CHP}	0.41	C_s^{CHP}	\$10/h
C_{OM}^{CHP}	\$5/h	$Ru_{\max}^{CHP}$	1500 kW/h
$Rd_{\max}^{CHP}$	1440 kW/h	$Q_{\max}^{boil}$	5385.7 kW
η^{boil}	0.8	C_s^{boil}	\$10/h
C_{OM}^{boil}	\$5/h	$Ru_{\max}^{boil}$	1000 kW/h
$Rd_{\max}^{boil}$	1529.2 kW/h	η^{HRU}	0.76
C_s^{HRU}	\$10/h	C_{OM}^{HRU}	\$5/h
$E_{\max}^{TS}$	1200 kWh	η_c^{TS}	0.9
η_d^{TS}	0.9	$Q_{\max}^{c}$	500 kW
$Q_{\max}^{d}$	500	C_s^{TS}	\$10/h
C_{OM}^{TS}	\$5/h	$E_{\max}^{ES}$	2013.3 kWh
η_c^{ES}	0.9	η_d^{ES}	0.9
$P_{\max}^{c}$	400 kW	$P_{\max}^{d}$	1000 kW
C_s^{ES}	\$10/h	C_{OM}^{ES}	\$5/h
$P_{\max}^{PV}$	933.3 kW	C_s^{PV}	\$10/h
C_{OM}^{PV}	\$5/h		

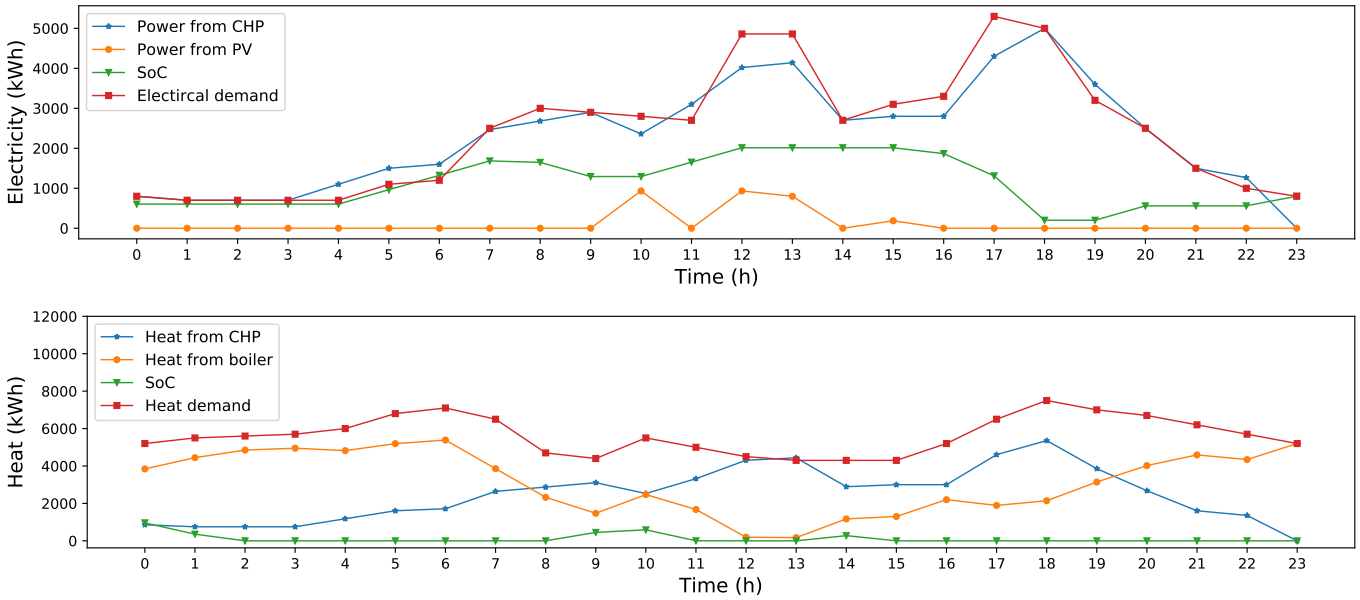

FIGURE 6: ELECTRICAL AND THERMAL DEMAND, PRODUCTION, STORAGE STATUS IN MGS UNDER DISRUPTION SCENARIOS.

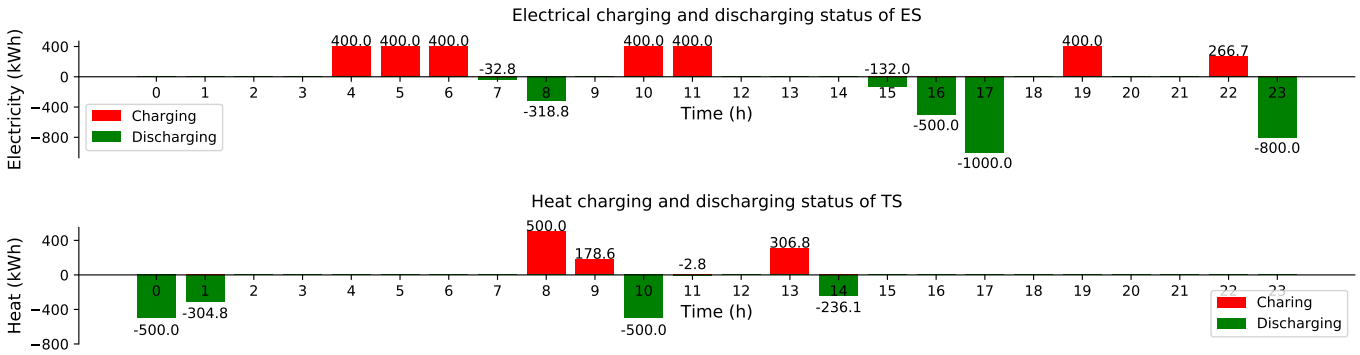

FIGURE 7: CHARGING AND DISCHARGING STATUS OF ES AND TS UNDER DISRUPTION SCENARIOS.

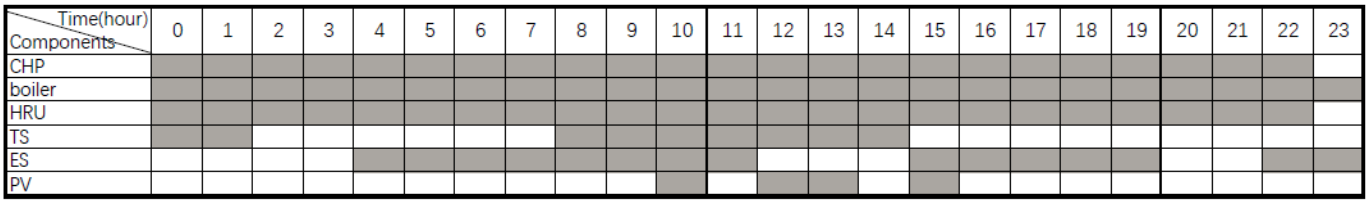

FIGURE 8: ON-OFF STATUS OF THE COMPONENTS UNDER DISRUPTION SCENARIOS.

TABLE 5: COSTS DIFFERENCES UNDER DISRUPTIVE AND NON-DISRUPTIVE SCENARIOS

Components	Disruptive C_{inst}	Non-disruptive C_{inst}	Increment	Disruptive C_{oper}	Non-disruptive C_{oper}	Increment
CHP	\$2,447.8	\$2,014.6	\$433.2	\$6,718.9	\$6,195.3	\$523.6
boiler	\$3,467.3	\$3,375.1	\$92.2	\$4,754.3	\$4,850.9	\$-96.6
HRU	\$594.8	\$666.7	\$-71.9	\$115	\$120	\$-5
TS	\$3,000	\$3,000	\$0	\$55	\$25	\$30
ES	\$3,353.5	\$3,248.6	\$104.9	\$105	\$90	\$15
PV	\$3,127	\$3,000	\$127	\$50	\$50	\$0
Total	\$15,990.4	\$15,305	\$685.4	\$11,798.2	\$11,331.2	\$467

As for the dynamic operational results, Fig. 6 shows the power and heat demand, the power and heat generation from the CHP, boiler, PV, and the SOC of the TS and ES throughout the simulation. All those results are derived from a CHP based MG, which consists of components with parameters shown in Table 4. The daily optimal operational cost C_{oper} is found to be $\$11,798.2$ for a system operating under disruptions. Figure 7 shows the charging and discharging status of the ES and TS. Figure 8 denotes the on-off status of the six components in the MG. Comparing to the on-off status of the components in the system without disruptions, the restarting becomes more frequent for all components except the boiler. And this difference is expected since the load and generation conditions become more complex with the presence of disruptions in the system. The generation and storage units require more flexibility to adjust their performances toward evolving operational conditions.

Although the online operations of each component change after introducing external disruptions to the MG, applying the design and operation control solutions derived from the optimization model not only satisfy the heat and power demand, but also minimizes the overall cost. The optimal total cost can be minimized to $\$27,788.6$.

After obtaining the solutions for the MG under non-disruptive and disruptive scenarios, the comparison between each component's operational and installation costs is shown in Table 5. It indicates that the increment in C_{inst} after injecting disruptions is mainly due to increasing C_{inst} of the CHP, boiler, ES and PV. And the higher C_{oper} is mainly because of the CHP unit in the case with disruptions. The total increment in C_{inst} and C_{oper} are \$685.4 and \$467, respectively, which only take up a small proportion of the original cost when no disruption occurs. However, if the same disruptive scenarios happen when all the components are designed according to Table 3, 7512kWh thermal and power demand will be unsatisfied after optimization, which can result in $\$300,480$ penalty cost. This amount of cost is above ten times higher than the total cost when considering disruptive scenarios, and therefore further proves the model's effectiveness in improving system's reliability. Additionally, Table 5 shows that the installation cost C_{inst} of the HRU, as well as the operational cost C_{oper} of the boiler and the HRU, even decrease in the case with disruptions. One reason for the difference in the cost of the system after considering disruptive events is that the design parameters need to be adjusted for any potential outage. For instance, the C_{inst} of the HRU decreases because the optimal heat recovery efficiency of HRU decreases from 0.8 to 0.76 to compensate for the additional heat provided by the TS, which is more flexible for the MG under outages. Besides, C_{oper} of the boiler becomes less because more heat is derived from the CHP instead of the boiler when electrical load increases by 80% between time steps $12-13$. Therefore, the cost of fuels from using the boiler decreases correspondingly. In conclusion, by adopting the co-optimization model, costs for both the operation controls and the design increase marginally after considering disruptive scenarios, because each component can be adjusted dynamically. As a result, the effectiveness of the developed co-design model is validated.

4. CONCLUSION

In this study, a co-design model for CHP-based MGs was presented. By formulating an MIP model, the system was optimized during both the operational and design stages. The paper mainly considers six components for the MG: the CHP, boiler, HRU, TS, ES, and PV units. When these components' characteristic parameters are determined, the optimal operational costs can be obtained by minimizing costs from from several folds: the production, operation/maintenance, startup, and unsatisfied load. Based on the power and heat demand, the optimal design parameters for each component can also be solved, and further, the optimal operational costs are calculated based on the components' optimal design. In this way, the proposed model can effectively find the optimal solution of the co-design problem.

The case study results demonstrated that considering disruptions would not significantly increase the costs from both operational and installation sides. The power and heat demands could always be satisfied even when some components have outages. However, ignore potential disruptions will result in a great loss from unsatisfied demand. These observations showed that the proposed co-design model could effectively attain the optimal design and system operation solutions for CHP-based MGs, and could cost-effectively improve the system's reliability and greatly reduced the losses caused by potential risks.

ACKNOWLEDGMENTS

This research is partially supported the U.S. Department of Energy's Office of Nuclear Energy under Award No. DE-NE0008899 and the National Science Foundation (NSF) Engineering Research Center for Power Optimization of Electro-Thermal Systems (POETS) with cooperative agreement EEC-1449548.

REFERENCES

[1] Twidell, John and Weir, Tony. *Renewable energy resources*. Routledge (2015).

[2] Vakulchuk, Roman, Overland, Indra and Scholten, Daniel. "Renewable energy and geopolitics: A review." *Renewable and Sustainable Energy Reviews* Vol. 122 (2020): p. 109547.

[3] Hinnells, Mark. "Combined heat and power in industry and buildings." *Energy Policy* Vol. 36 No. 12 (2008): pp. 4522–4526. DOI https://doi.org/10.1016/j.enpol.2008.09.018. URL https://www.sciencedirect.com/science/article/pii/S0301421508004758. Foresight Sustainable Energy Management and the Built Environment Project.

[4] Andrews, D. "'Carbon footprints of various sources of heat—Biomass combustion and CHPDH comes out lowest." *William Orchard. Claverton Energy Research Group. http://www. clavertonenergy. com/carbon-footprints-of-various-sources-of-heat-chpdh-comesout-lowest. html. Accessed April* Vol. 1 (2009): p. 2013.

[5] Gvozdenac, Dušan, Urošević, Branka Gvozdenac, Menke, Christoph, Urošević, Dragan and Bangviwat, Athikom. "High efficiency cogeneration: CHP and non-CHP energy." *Energy* Vol. 135 (2017): pp. 269–278.

[6] Darrow, Ken, Tidball, Rick, Wang, James, Hampson, Anne et al. "Catalog of CHP technologies." *US Environmental Protection Agency Combined Heat and Power Partnership* .

[7] Gbadamosi, Saheed Lekan and Nwulu, Nnamdi I. "Optimal power dispatch and reliability analysis of hybrid CHP-PV-wind systems in farming applications." *Sustainability* Vol. 12 No. 19 (2020): p. 8199.

[8] Adhvaryyu, Shreya and Adhvaryyu, Pradosh Kumar. "Application of bio-inspired social spider algorithm in multi-area economic emission dispatch of solar, wind and CHP-based power system." *Soft Computing* Vol. 24 No. 13 (2020): pp. 9611–9624.

[9] Mahian, Omid, Javidmehr, Mohammad, Kasaeian, Alibakhsh, Mohasseb, Sassan and Panahi, Mouzhan. "Optimal sizing and performance assessment of a hybrid combined heat and power system with energy storage for residential buildings." *Energy Conversion and Management* Vol. 211 (2020): p. 112751.

[10] Hu, Junyan and Lanzon, Alexander. "Distributed finite-time consensus control for heterogeneous battery energy storage systems in droop-controlled microgrids." *IEEE Transactions on smart grid* Vol. 10 No. 5 (2018): pp. 4751–4761.

[11] Hannan, MA, Tan, Shun Y, Al-Shetwi, Ali Q, Jern, Ker Pin and Begum, RA. "Optimized controller for renewable energy sources integration into microgrid: Functions, constraints and suggestions." *Journal of Cleaner Production* Vol. 256 (2020): p. 120419.

[12] Ibrahim, Marwa et al. "Optimization of Renewable Energy-Based Smart Micro-Grid System." *Chapters* .

[13] Komala, K., Kumar, K. Prakash and Cherukuri, S. Hari Charan. "Storage and non-Storage Methods of Power balancing to counter Uncertainty in Hybrid Microgrids - A review." *Journal of Energy Storage* Vol. 36 (2021): p. 102348. DOI https://doi.org/10.1016/j.est.2021.102348. URL https://www.sciencedirect.com/science/article/pii/S2352152X21001110.

[14] Nazari-Heris, Farhad, Mohammadi-ivatloo, Behnam and Nazarpour, D. "Network constrained economic dispatch of renewable energy and CHP based microgrids." *International Journal of Electrical Power & Energy Systems* Vol. 110 (2019): pp. 144–160.

[15] Mirzaei, Mohammad Amin, Sadeghi-Yazdankhah, Ahmad, Mohammadi-Ivatloo, Behnam, Marzband, Mousa, Shafiekhah, Miadreza and Catalão, João PS. "Integration of emerging resources in IGDT-based robust scheduling of combined power and natural gas systems considering flexible ramping products." *Energy* Vol. 189 (2019): p. 116195.

[16] Gholinejad, Hamid Reza, Loni, Abdolah, Adabi, Jafar and Marzband, Mousa. "A hierarchical energy management system for multiple home energy hubs in neighborhood grids." *Journal of Building Engineering* Vol. 28 (2020): p. 101028.

[17] Martinez, Simon, Michaux, Ghislain, Salagnac, Patrick and Bouvier, Jean-Louis. "Micro-combined heat and power systems (micro-CHP) based on renewable energy sources." *Energy Conversion and Management* Vol. 154 (2017): pp. 262–285.

[18] Masrur, Hasan, Khan, Kaisar R, Abumelha, Waleed and Senjyu, Tomonobu. "Efficient energy delivery system of the CHP-PV based microgrids with the economic feasibility study." *International Journal of Emerging Electric Power Systems* Vol. 21 No. 1.

[19] Wang, Yi, Rousis, Anastasios Oulis and Strbac, Goran. "On microgrids and resilience: A comprehensive review on modeling and operational strategies." *Renewable and Sustainable Energy Reviews* Vol. 134 (2020): p. 110313.

[20] Yodo, Nita and Wang, Pingfeng. "Engineering resilience quantification and system design implications: A literature survey." *Journal of Mechanical Design* Vol. 138 No. 11.

[21] Yodo, Nita and Wang, Pingfeng. "Resilience modeling and quantification for engineered systems using Bayesian networks." *Journal of Mechanical Design* Vol. 138 No. 3.

[22] Yodo, Nita and Wang, Pingfeng. "Resilience allocation for early stage design of complex engineered systems." *Journal of Mechanical Design* Vol. 138 No. 9.

[23] Yodo, Nita, Wang, Pingfeng and Rafi, Melvin. "Enabling resilience of complex engineered systems using control theory." *IEEE Transactions on Reliability* Vol. 67 No. 1 (2017): pp. 53–65.

[24] Yodo, Nita, Wang, Pingfeng and Zhou, Zhi. "Predictive resilience analysis of complex systems using dynamic Bayesian networks." *IEEE Transactions on Reliability* Vol. 66 No. 3 (2017): pp. 761–770.

[25] Yodo, Nita and Wang, Pingfeng. "A control-guided failure restoration framework for the design of resilient engineering systems." *Reliability Engineering & System Safety* Vol. 178 (2018): pp. 179–190.

[26] Hu, Chao, Youn, Byeng D and Wang, Pingfeng. "Reliability-Based Design Optimization." *Engineering Design under Uncertainty and Health Prognostics*. Springer (2019): pp. 187–231.

[27] Wu, Jiaxin and Wang, Pingfeng. "A comparison of control strategies for disruption management in engineering design for resilience." *ASCE-ASME J Risk and Uncert in Engrg Sys Part B Mech Engrg* Vol. 5 No. 2.

[28] Wu, Jiaxin and Wang, Pingfeng. "Risk-Averse Optimization for Resilience Enhancement of Complex Engineering Systems under Uncertainties." *arXiv preprint arXiv:2009.02351* .

[29] Wu, Jiaxin and Wang, Pingfeng. "Post-disruption performance recovery to enhance resilience of interconnected network systems." *Sustainable and Resilient Infrastructure* (2020): pp. 1–17.

[30] Zafarani, Hamidreza, Taher, Seyed Abbas and Shahidehpour, Mohammad. "Robust operation of a multicarrier energy system considering EVs and CHP units." *Energy* Vol. 192 (2020): p. 116703.

[31] Odonkor, Philip and Lewis, Kemper. "Automated design of energy efficient control strategies for building clusters using reinforcement learning." *Journal of Mechanical Design* Vol. 141 No. 2.

[32] Odonkor, Philip and Lewis, Kemper. "Data-Driven Design of Control Strategies for Distributed Energy Systems." *Journal of Mechanical Design* Vol. 141 No. 11.

[33] Olympios, Andreas V, Pantaleo, Antonio M, Sapin, Paul and Markides, Christos N. "On the value of combined heat and power (CHP) systems and heat pumps in centralised and distributed heating systems: Lessons from multi-fidelity modelling approaches." *Applied Energy* Vol. 274 (2020): p. 115261.

[34] Lu, Shen, Schroeder, Nathan B, Kim, Harrison M and Shanbhag, Uday V. "Hybrid power/energy generation through multidisciplinary and multilevel design optimization with complementarity constraints." *Journal of Mechanical Design* Vol. 132 No. 10.

[35] Allison, James T, Guo, Tinghao and Han, Zhi. "Co-design of an active suspension using simultaneous dynamic optimization." *Journal of Mechanical Design* Vol. 136 No. 8.

[36] Cui, Tonghui, Allison, James T and Wang, Pingfeng. "A comparative study of formulations and algorithms for reliability-based co-design problems." *Journal of Mechanical Design* Vol. 142 No. 3.

[37] Nash, Austin L and Jain, Neera. "Hierarchical Control Co-Design Using a Model Fidelity-Based Decomposition Framework." *Journal of Mechanical Design* Vol. 143 No. 1.

[38] Liu, Tianchen, Azarm, Shapour and Chopra, Nikhil. "Decentralized Multisubsystem Co-Design Optimization Using Direct Collocation and Decomposition-Based Methods." *Journal of Mechanical Design* Vol. 142 No. 9.

[39] Padberg, Manfred and Rinaldi, Giovanni. "A branch-and-cut algorithm for the resolution of large-scale symmetric traveling salesman problems." *SIAM review* Vol. 33 No. 1 (1991): pp. 60–100.

[40] Optimization, Gurobi. "Inc.,"Gurobi optimizer reference manual," 2015." (2014).

[41] Romero-Quete, David and Garcia, Javier Rosero. "An affine arithmetic-model predictive control approach for optimal economic dispatch of combined heat and power microgrids." *Applied Energy* Vol. 242 (2019): pp. 1436–1447.

[42] Nojavan, Sayyad, Akbari-Dibavar, Alireza, Farahmand-Zahed, Amir and Zare, Kazem. "Risk-constrained scheduling of a CHP-based microgrid including hydrogen energy storage using robust optimization approach." *International Journal of Hydrogen Energy* Vol. 45 No. 56 (2020): pp. 32269–32284.

[43] Patro, S and Sahu, Kishore Kumar. "Normalization: A preprocessing stage." *arXiv preprint arXiv:1503.06462* .

[44] Navarro, Juan Pablo Jiménez, Kavvadias, Konstantinos C, Quoilin, Sylvain and Zucker, Andreas. "The joint effect of centralised cogeneration plants and thermal storage on the efficiency and cost of the power system." *Energy* Vol. 149 (2018): pp. 535–549.

[45] Chittum, Anna and Relf, Grace. "Valuing distributed energy resources: Combined heat and power and the modern grid." *The Electricity Journal* Vol. 32 No. 1 (2019): pp. 52–57.

[46] Kia, Mohsen, Nazar, Mehrdad Setayesh, Sepasian, Mohammad Sadegh, Heidari, Alireza and Siano, Pierluigi. "Optimal day ahead scheduling of combined heat and power units with electrical and thermal storage considering security constraint of power system." *Energy* Vol. 120 (2017): pp. 241–252.

[47] Wang, Kai, Pantaleo, Antonio M, Herrando, María, Faccia, Michele, Pesmazoglou, Ioannis, Franchetti, Benjamin M and Markides, Christos N. "Spectral-splitting hybrid PV-thermal (PVT) systems for combined heat and power provision to dairy farms." *Renewable Energy* Vol. 159 (2020): pp. 1047–1065.